

## Polymeric micromechanical components with tunable stiffness

E. Manias, J. Chen, N. Fang, and X. Zhang

Citation: [Applied Physics Letters](#) **79**, 1700 (2001); doi: 10.1063/1.1400084

View online: <http://dx.doi.org/10.1063/1.1400084>

View Table of Contents: <http://scitation.aip.org/content/aip/journal/apl/79/11?ver=pdfcov>

Published by the [AIP Publishing](#)

---

### Articles you may be interested in

[Origin of bending in uncoated microcantilever - Surface topography?](#)

Appl. Phys. Lett. **104**, 041602 (2014); 10.1063/1.4863675

[Polymer microcantilevers fabricated via multiphoton absorption polymerization](#)

Appl. Phys. Lett. **86**, 064105 (2005); 10.1063/1.1863414

[Fatigue life of a microcantilever beam in bending](#)

J. Vac. Sci. Technol. B **22**, 3143 (2004); 10.1116/1.1821502

[Adhesion force of polymeric three-dimensional microstructures fabricated by microstereolithography](#)

Appl. Phys. Lett. **81**, 3963 (2002); 10.1063/1.1522825

[Fabrication of submicron suspended structures by laser and atomic force microscopy lithography on aluminum combined with reactive ion etching](#)

J. Vac. Sci. Technol. B **16**, 2977 (1998); 10.1116/1.590329

---



## Polymeric micromechanical components with tunable stiffness

E. Manias<sup>a)</sup> and J. Chen

*Materials Science and Engineering, Penn State University, University Park, Pennsylvania 16802*

N. Fang and X. Zhang

*Mechanical and Aerospace Engineering, University of California, Los Angeles, Los Angeles, California 90095*

(Received 21 May 2001; accepted for publication 13 July 2001)

We present a microstereolithographic technique that enables the manufacturing of polymeric components for microelectromechanical systems. Model microstructures were fabricated in the form of end-supported microbeams (10  $\mu\text{m}$  in diameter), in order to characterize the mechanical properties of the produced structures at the micron scale. The flexural modulus of these microbeams was measured by atomic force microscopy, using cantilevers with attached metal spheres, and employed in a three-point bending geometry. Postfabrication treatment of the microstructures allows for the tailoring of their stiffness. © 2001 American Institute of Physics.

[DOI: 10.1063/1.1400084]

An increasingly strong interest for the development of micromachining technology has driven a rapidly growing research effort in microelectromechanical systems (MEMS) in the last decade. These microsystems involve integrated sensing and actuating elements with sophisticated shape and functions. The need to manufacture such diverse elements oftentimes necessitates utilizing materials that are beyond conventional integrated circuit (IC) fabrication, and consequently compels alternative microfabrication techniques. Microstereolithography ( $\mu\text{SL}$ ), for example, adopted from the stereolithographic process in rapid prototyping, turns out to be a viable candidate in this area, both for polymeric and ceramic materials.<sup>1</sup>  $\mu\text{SL}$  enables the manufacturing of complex three-dimensional (3D) shapes, by means of localized photopolymerization via a sharply focused laser beam, with a lateral resolution of 1–1.2  $\mu\text{m}$  on the defined structures.<sup>1</sup>

The mechanical properties of microstructures are a critical factor in the performance and reliability of MEMS devices, and thus important for microfabrication technology. In numerous cases, catastrophic failure of microactuated devices occurs when surfaces impact—either unintentionally or as a part of the normal device operation—and components suffer permanent damage. Reducing the stiffness of such components will facilitate their survival. At the same time, the same MEMS components should have high enough modulus to enable the efficient transfer of forces from one element to another. Consequently, it would be of great importance to develop a method that can produce well-defined MEMS elements with controlled stiffness and strength, as dictated by design principles.

Stereolithography does provide this capability at the macroscopic scale. For example, tensile tests of macroscopic specimens made by stereolithographic processes showed that the modulus and strength of photocured polymer parts varies with laser intensity and scanning speed.<sup>2</sup> However, there is no evidence yet that this is also the case in any of the microstructures formed by  $\mu\text{SL}$  process. One of the reasons that

this area is yet to be explored is the lack of reliable methods to quantitatively measure the modulus and strength of  $\mu\text{SL}$ -fabricated micron-scale structures. Several atomic force microscopy (AFM) methods have been developed to study the surface stiffness,<sup>3</sup> as well as to obtain information about the elasticity over depths of a few nanometers by probe indentation.<sup>4</sup> However, these methods are not suitable to interrogate the mechanical properties of materials at scales relevant to the MEMS components (i.e., several microns).

Therefore, it is our objective in this work to devise an AFM method that provides the ability of probing mechanical properties at the microscale, especially in relation to  $\mu\text{SL}$  fabricated polymer microstructures. Furthermore, by studying model  $\mu\text{SL}$  microstructures, we want to explore possible pathways to fabricate microstructures of tunable stiffness without changing geometric designs.

From this viewpoint, we studied the modulus of end-supported polymer beams (Fig. 1) defined by the  $\mu\text{SL}$  process, in the green state (as produced by the  $\mu\text{SL}$ ), and after subsequent postfabrication curing. This geometry mimics the macroscopic three-point-flexure tensile test (e.g., Sec. 2.IIa in Ref. 5) at the micron scale. The samples of polymer microbeams are manufactured on a microstereolithographic system developed recently, and described in detail elsewhere.<sup>1</sup> The system involves an  $\text{Ar}^+$  laser with 364 nm output—aligned with related beam delivery and focusing optics—and a precision  $x$ - $y$ - $z$  translation stage.<sup>1</sup> A 3D shape designed with computer-aided design (CAD) software is sliced into a series of two-dimensional (2D) layers with uniform thickness, typically, about 10  $\mu\text{m}$ , which are realized in polymer by using a sharply focused UV laser to selectively polymerize a photocurable solution. The focused UV spot (1–5  $\mu\text{m}$ ) is scanned in a layer-by-layer fashion to form complex 3D microstructures, according to the CAD-defined pattern. The submicron control of the  $x$ - $y$ - $z$  translation stage in conjunction with the fine UV beam spot enables the precise fabrication of 3D microstructures, with a resolution of 1.2  $\mu\text{m}$ , and shapes that range from microgears, to high-aspect-ratio microtubes, and 3D microchannels.<sup>1</sup>

<sup>a)</sup>Author to whom correspondence should be addressed; electronic mail: manias@psu.edu

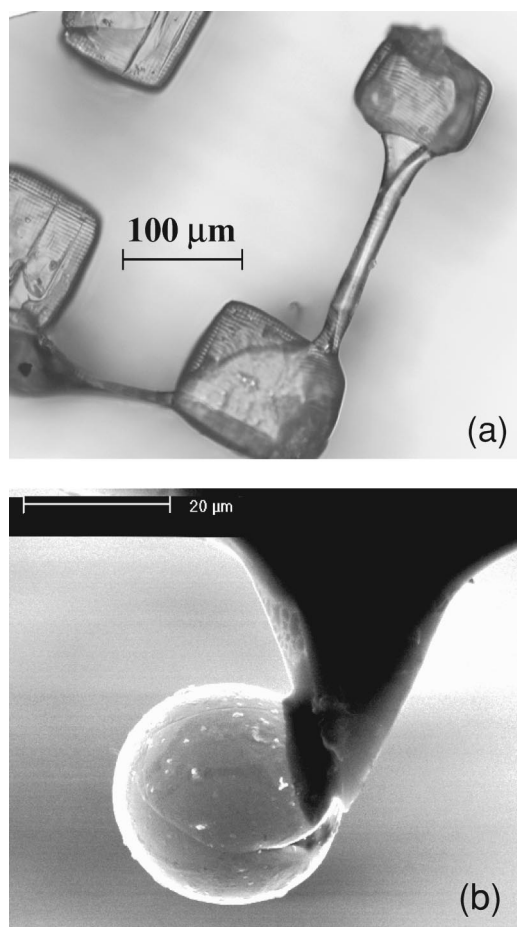


FIG. 1. (a) Typical 10- $\mu\text{m}$ -diam beam used for modulus measurements, in this case, of length 200  $\mu\text{m}$ . (b) SEM of a typical sphere-bearing AFM tip.

Implementation of a two-photon adsorption process can attain submicron  $\mu\text{SL}$  resolution.<sup>6</sup>

The UV polymerizable solution in this work is comprised of a mixture of monomer [1,6-hexanediol diacrylate (HDDA)], [ $\text{H}_2\text{C}=\text{CHCO}_2(\text{CH}_2)_3-$ ]<sub>2</sub>, (Aldrich), and photoinitiator [benzoin ethyl ether, (BEE)], [ $\text{C}_6\text{H}_5\text{CH}(\text{OC}_2\text{H}_5)\text{COC}_6\text{H}_5$ ], (Aldrich). In order to control the penetration depth of light within the resin, a commercial UV absorber is also added (Tinuvin™ 234 from Ciba Specialty Chemicals Corp). The 3D polymer microstructures are defined by  $\mu\text{SL}$  on silicon substrates. Several cylindrical beams, of cac. 10  $\mu\text{m}$  in diameter, are supported on both ends by two identical posts 300  $\mu\text{m}$  in height, and  $100 \times 100 \mu\text{m}$  in lateral dimensions. We varied the length of the supported microbeams from 100 to 600  $\mu\text{m}$ . The laser scanning speed and light intensity were varied so as to achieve the optimal shape definition for reasonable processing time (for the supporting posts: 166  $\mu\text{m}/\text{s}$  and  $5 \times 10^5 \text{ W}/\text{m}^2$  respectively, while for the microbeams: 16.6–33.3  $\mu\text{m}/\text{s}$  at  $2.6 \times 10^4 \text{ W}/\text{m}^2$ ).

When such an end-supported cylindrical beam (Fig. 1) is loaded at its middle, the flexural/elastic modulus ( $E$ ) can be quantified by the central deflection ( $Y$ ) under an applied force ( $F$ ) (Fig. 2), through:

$$E = \frac{4FL_o^3}{3\pi D^4 Y} \quad (1)$$

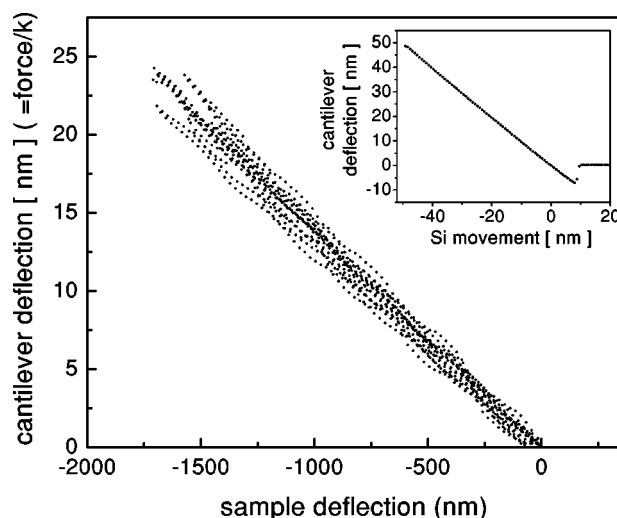


FIG. 2. Flexural test of the 200  $\mu\text{m}$  beam at the green state, by a cantilever of  $k = 58.2 \text{ N}/\text{m}$  bearing a 25.1  $\mu\text{m}$  diam W sphere (12 different approaches, raw data). Inset: the same tip–sphere system on Si.

where  $L_o$  is the cylinder length at rest, and  $D$  its diameter (Fig. 3, inset).<sup>5</sup> In order to measure the mechanical properties of the micrometer structure, it is necessary for the whole cylinder to undergo a mechanical deformation. AFM is ideally suited for these measurements, as it provides a simultaneous measurement of the applied force and the sample deformation, at the relevant force and length scales. However, the use of a conventional sharp AFM tip would limit our ability to bend the whole microcylinder (since the nanometer-sharp tip indents the microstructure surface much before it can apply high enough forces to bend the 10- $\mu\text{m}$ -diam beams). To this end, we have modified conventional AFM cantilevers (Silicon MDT) by affixing<sup>7</sup> large tungsten spheres on their tips (sphere diameter, 20–25  $\mu\text{m}$ , Fig. 1). These micron-sized spheres enable us to probe the microstructure with high enough forces so as to bend the beam by 0.5–1.5  $\mu\text{m}$ ; at the same time, the added sphere mass provides for an easy and accurate calibration of the AFM cantilever spring constant.<sup>8</sup> The precise knowledge of the cantilever spring constant is crucial for the quantitative evaluation of the applied force. Moreover, for the measurements herein stiff cantilevers are required, and for this reason we evaporate on commercial contact cantilevers thin chromium films setting the cantilever stiffnesses between 50 and 150 N/m.

The approach of our AFM studies is similar to that of indentation or force–distance experiments: We position the AFM sphere-bearing tip above the center of the end-supported cylindrical rod. Using the force–distance AFM mode, the tip/sphere approaches the rod until it comes in contact at zero applied normal force. Subsequently, we exert a normal force on the cylinder which bends downwards. During the experiment the deformation of the beam and the tip deflection are simultaneously measured (Fig. 2); the latter can be translated into the applied normal force (via the known cantilever spring constant). Such a stress–strain measurement is shown in Fig. 2, for the 200  $\mu\text{m}$  beam (as shown in Fig. 1) probed by a 25  $\mu\text{m}$  sphere-bearing AFM tip. We require at least 1  $\mu\text{m}$  of central deflection (sample deformation) for the 10- $\mu\text{m}$ -diameter rods studied. For each rod three different cantilevers were used to obtain 12 force–distance

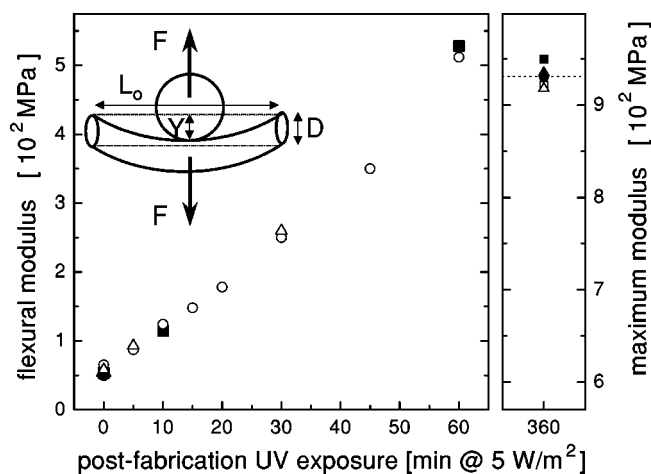


FIG. 3. Measured flexural moduli for two beams  $200\ \mu\text{m}$  (filled symbols) and  $400\ \mu\text{m}$  (open symbols) vs postfabrication curing. Different symbols correspond to experiments with different cantilevers. The modulus of the fully cured microbeam (right) is  $930 \pm 12\ \text{MPa}$ . Inset: the geometry used for the modulus measurement [symbols as per Eq. (1)].

measurements each. The elastic moduli obtained were very reproducible across all measurements, which is not surprising given that we study forces and lengths three orders of magnitude larger than the AFM resolution.

The modulus of the rods is measured at the green state (as obtained from the  $\mu\text{SL}$ ), as well as after further exposure to UV radiation. The flexural moduli versus postfabrication curing times are given in Fig. 3, where the elastic modulus is shown to increase from its initial value at the green state to a maximum value of  $930 \pm 12\ \text{MPa}$  with postfabrication curing. As expected,<sup>1</sup> after the  $\mu\text{SL}$  fabrication there still remain unreacted sites within the device. Further exposure to UV radiation drives the polymerization reaction to completion, thus gradually increasing the elastic modulus, and eventually attaining a value comparable to the corresponding bulk modulus. The bulk modulus value is reached because the beam size (tens of  $\mu\text{m}^3$ ) is far too big for any molecular nature of the material to manifest itself in its mechanical response. The maximum modulus is characteristic of the materials used and the layer-thickness/pitch chosen during the  $\mu\text{SL}$  ( $10\ \mu\text{m}$ , in our case).<sup>1</sup> Thus, postfabrication curing en-

ables us to selectively choose the modulus in a range defined by the modulus at the green state and its bulk value. This ability to tailor the elastic modulus of the microstructure combined with recent advances of ultrastrong (siloxane-coaliphatic) UV-curable epoxy polymers,<sup>9</sup> enables the design of polymeric MEMS elements with moduli selected on demand from a range of 50 MPa–20 GPa, and accompanying strengths.

In summary, we describe an approach to manufacture polymeric MEMS components of tailored modulus. Model microstructures were fabricated, via microstereolithography ( $\mu\text{SL}$ ) from a UV-polymerizable precursor, and their moduli were measured by AFM. As produced by the  $\mu\text{SL}$  the microstructures are characterized by low flexural moduli, but via postfabrication exposure to UV radiation their stiffness can be increased up to the bulk modulus. Selection of a stiffer cross-linkable system can expand the range of feasible moduli from 50 MPa to 20 GPa.

The AFM instrumentation was supported by NSF under Grant No. DMR 9975624.

- <sup>1</sup>X. Zhang, X. Jiang, and C. Sun, *Sens. Actuators A* **77**, 149 (1999).
- <sup>2</sup>C. M. Cheah, A. Nee, J. Fuh, L. Lu, Y. S. Choo, and T. Miyazawa, *J. Mater. Process. Technol.* **67**, 41 (1997); **67**, 47 (1997).
- <sup>3</sup>S. Akari, E. vdVegte, P. C. M. Grim, G. F. Belder, V. Koutsos, G. ten Brinke, and G. Hadziioannou, *Appl. Phys. Lett.* **65**, 1915 (1994); J. Domke and M. Radmacher, *Langmuir* **14**, 3320 (1998); *ibid.* **13**, 2825 (1997); D. deVecchio and B. Bhushan, *Rev. Sci. Instrum.* **68**, 4498 (1997); S. Chizhik, Z. Huang, V. Gorbunov, N. Myshkin, and V. Tsukruk, *Langmuir* **14**, 2606 (1998); C. Basire and C. Fetigny, *Eur. Phys. J.: Appl. Phys.* **6**, 323 (1999).
- <sup>4</sup>C. Fetigny, C. Basire, and V. Granier, *J. Appl. Phys.* **82**, 43 (1997); S. Chizhik, Z. Huang, V. Gorbunov, N. Myshkin, and V. V. Tsukruk, *Langmuir* **14**, 2606 (1998); D. Gracias and G. Somorjai, *Macromolecules* **31**, 1269 (1998); B. Akhremitchev and G. Walker, *Langmuir* **15**, 5630 (1999).
- <sup>5</sup>L. Nielsen and R. Landel, *Mechanical Properties of Polymers and Composites* (Marcel Dekker, New York, 1994).
- <sup>6</sup>H. Sun, S. Matsuo, and H. Misawa, *Appl. Phys. Lett.* **74**, 786 (1999).
- <sup>7</sup>We have used a high modulus epoxy to fix the tungsten spheres on the AFM tips. The modulus of the epoxy was tested by force–distance AFM against Si wafers, where the epoxy did not deform even at the highest cantilever deflections (Fig. 2, inset).
- <sup>8</sup>J. Cleveland, S. Manne, D. Bocek, and P. Hansma, *Rev. Sci. Instrum.* **64**, 1868 (1993).
- <sup>9</sup>S. Kong and J. Crivello, *Polym. Prepr. (Am. Chem. Soc. Div. Polym. Chem.)* **40**, 569 (1999).